## Title
An analytical approach for estimating CO2 and heat fluxes over the Amazonian region



## Journal
Ecological Modelling, 162(1-2)

## ISSN
0304-3800

## Authors
Zhan, X W
Xue, Yongkang K
Collatz, G J

## Publication Date
2003-04-01

Peer reviewed

ELSEVIER

Ecological Modelling 3231 (2002) 1–21

ECOLOGICAL MODELLING

www.elsevier.com/locate/ecolmodel

# An analytical approach for estimating $CO_2$ and heat fluxes over the Amazonian region

Xiwu Zhan [a,*], Yongkang Xue [b], G. James Collatz [c]

[a] *UMBC-GEST/NASA-GSFC Hydrological Science Branch, Code 974.1, Greenbelt, MD 20771, USA*
[b] *Department of Geography, UCLA, Los Angeles, CA, USA*
[c] *Goddard Space Flight Center, Code 923, Greenbelt, MD, USA*

Received 17 April 2002; received in revised form 23 October 2002; accepted 20 November 2002

**Abstract**

Accurate assessments of the $CO_2$ fluxes between the terrestrial ecosystems and the atmosphere are pressingly needed for the climate change and carbon cycle studies. The Collatz et al. parameterization of leaf photosynthesis-stomatal conductance has been widely applied in land surface parameterization schemes for simulating the land surface $CO_2$ fluxes. The study in this paper developed an analytical solution approach for the Collatz et al.'s parameterization for stable solution and computational efficiency. This analytical approach is then applied to the simplified biosphere model (SSiB), enhancing its capability of simulating land surface $CO_2$ fluxes. The enhanced SSiB model is tested with field observation data sets from two Amazonian field experiments (ABRACOS missions and Manaus Eddy Covariance Study). Simulations of the land surface fluxes of latent heat, sensible heat and soil heat by the enhanced SSiB agree very well with observations with correlation coefficients being larger than 0.80. However, the correlation coefficient for the daily means of $CO_2$ fluxes is only 0.42 for the Manaus data set. A day-time "square wave" in the simulated $CO_2$ flux diurnal curves is found. The discrepancies between simulation and observation were found to be the results of incorrect parameter setup or improper leaf to canopy scaling strategy. A modification to the scaling strategy improves significantly the accuracy of the photosynthesis-stomatal conductance model.


*Keywords:* Photosynthesis; Stomatal conductance; $CO_2$; Energy balance; Simplified biosphere model (SSiB); Analytical solution; ABRACOS; LBA

## 1. Introduction

Since the late 1970s, numerical modeling experiments using the coupled atmospheric and land surface models have been carried out to explore the relationship between land surface characteristics and the global as well as regional climate. These studies have shown that the changes in land surface characteristics, such as albedo, surface roughness length, vegetation properties, and soil properties, could substantially alter terrestrial hydrologic system at global and regional scales (see reviews by Sellers et al., 1997; Kabat and Claaussen, 2002). In these studies, biophysical models with different complexity have been developed. The project for intercomparison of land-surface parameterization scheme (PILPS, Henderson-Seller et al., 1993, 1995) has also been carried out to evaluate and improve the land surface parameterizations, and, therefore, to enhance the models' ability predicting the water cycle. In these models, however, empirical work

* Corresponding author. Tel.: +1-301-286-3885; fax: +1-603-806-8375.
*E-mail address:* xzhan@hab.gsfc.nasa.gov (X. Zhan).

0304-3800/02/$ – see front matter © 2002 Published by Elsevier Science B.V.
doi:10.1016/S0304-3800(02)00405-2

had correlated stomatal conductance to the environmental conditions independent from any consideration of photosynthesis. By the late 1980s, scientific interest on global change, particularly on the "greenhouse effect" had promoted the development of more complete models, which directly couple water and carbon cycle processes (Sellers et al., 1997).

Increase in greenhouse gases, in particular $CO_2$, has great impacts on global climate change. The potential importance of land carbon cycle to the global climate was suggested in Cox et al. (2000) who performed future climate simulations with interactive vegetation and ocean carbon cycles. Their simulations produced significant climate warming caused by climate-induced loss of Amazonian rainforests. Recent studies have shown that terrestrial ecosystems, especially tropical rain forest, may be an important sink of atmospheric $CO_2$ (Tian et al., 2000; Schimel et al., 2001). Regional studies based on in situ measurements are consistent with carbon sinks associated with tropical forests (Phillips et al., 1998). The Amazon region contains the largest area of tropical forest on Earth. Over the past 25 years, rapid development has led to the destruction of over 500,000 $km^2$ of forest in Brazil (Houghton et al., 2000), producing a large source for atmospheric $CO_2$. Study has found that the Amazonian region acted as a net source for carbon in a range of 0.2–1.2 Pg $year^{-1}$ from 1992 to 1993 mainly because of the deforestation (Keller et al., 2001). Since emissions from land clearing in the tropics are thought to be large, there must be offsetting sinks to balance these emissions. All of these indicate a pressing need for accurate assessments of the $CO_2$ fluxes between the terrestrial ecosystems and the atmosphere.

Two efforts are required to address this need: one is the observation of $CO_2$ fluxes between a terrestrial ecosystem and the atmosphere in field for ground truth; and the other is the development and validation of models to understand the observed evidence and to extrapolate the modeling results to the other regions. The first effort has been made in many large-scale field experiments, one of which is the Large-Scale Biosphere-Atmosphere Experiment in Amazonia (LBA, Keller et al., 1997). A number of other field data sets have been collected in this region for analyses and model validation. In the study of this paper, the data from Anglo-Brazilian Amazonian Climate Observation Study (ABRACOS, Gash et al., 1996) and another measurement in central Amazonian rain forest (Malhi et al., 1998) are used.

In addition to field measurement, great deal of effort has been carried out to develop plant photosynthesis models since 1970s (Thornley and Johnson, 1990) and has gained more attention from the ecological science (Jorgensen, 1997) and climate modeling communities (Sellers et al., 1992). This model development effort is still going on (Boonen et al., 2002). Collatz et al. (1991, 1992) combined the biochemical photosynthesis model in Farquhar et al. (1980) with the semi-empirical stomatal conductance model of Ball (1988) to estimate stomatal conductance and photosynthesis rate of leaves simultaneously. We will refer Collatz et al. parameterization of leaf photosynthesis-stomatal conductance as Collatz et al. model in this paper. Taking advantages of its strong physical and biochemical bases, Sellers et al. (1996a) adapted this coupled photosynthesis-stomatal conductance model in the revised Simple Biosphere model (SSiB_2) for simulating land surface energy and $CO_2$ fluxes by scaling up leaf responses to the canopy level. The SSiB_2 model has been applied in global climate and carbon cycle studies (Sellers et al., 1996a,b; Sellers et al., 1997; Denning et al., 1996a,b). However, the iterative solution used in the photosynthesis-stomatal conductance model is computationally expensive and also may become numerically unstable under certain environmental conditions (Baldocchi, 1994). Proper procedure must be taken to avoid such circumstances. In contrast, an analytical solution for the coupled leaf photosynthesis-stomatal conductance model can avoid these problems.

Baldocchi (1994) made an early attempt to derive an analytical solution of the leaf photosynthesis equations in Farquhar et al. (1980) and stomatal conductance in Ball (1988). The equations used in Baldocchi (1994) are similar to those in Collatz et al. (1991), but they differ from those in Sellers et al. (1996a), which includes scaling from leaf to vegetation canopies. In addition, the version of the Collatz et al.' model in Sellers et al. (1996a) considers broader environmental conditions. For example, the photosynthesis equations of Collatz' coupled model in Sellers et al. (1996a) takes accounts of three photosynthetic limitations rather than the two photosynthetic limitations considered by Baldocchi (1994). Thus, an analytical approach for the Collatz'

coupled model in Sellers et al. (1996a) should be different from those in Baldocchi (1994). Because of the wide applications of the Collatz et al. model (Bonan, 1995; Sellers et al., 1996a,b; Denning et al., 1996a,b; Chen et al., 1999), deriving its analytical solutions of the more complex form should provide a useful approach for the global climate and carbon cycling studies.

The simplified biosphere model (SSiB) of Xue et al. (1991) has been evaluated by observational data from different vegetation types and different geographical location, and has been broadly used in global and regional climate studies, including the LBA (for example, Xue et al., 1996a; Chou et al., 2002). However, the current version of SSiB uses Jarvis' empirical approach (Jarvis, 1976) for the formulation of stomatal conductance. It does not consider the photosynthetic activities of land surface vegetation and is thus unable to estimate land surface $CO_2$ fluxes for carbon cycling studies. In this paper, we attempt to enhance the SSiB model by deriving an analytical solution from Collatz et al. model and to apply it to SSiB. Replacing the empirical stomatal resistance submodel in SSiB with Collatz et al. model, the SSiB model is then revised to have the $CO_2$ flux simulation capability. To test this extended capability of the SSiB model as a part of our effort within the LBA frame, we ran the model with the observational data from two large-scale field experiments held in Amazonian tropical forests. The output from the model is analyzed against their corresponding field observations. Discrepancies between simulation and observation were found as a result of incorrect parameter setup or improper leaf to canopy scaling strategy. A modification to the scaling strategy improves significantly the accuracy of the photosynthesis-stomatal conductance model. Finally, further improvement of the revised SSiB model is discussed. It is important to note that the net $CO_2$ flux from the land surface is a function of both photosynthetic uptake and respiratory release by plants and decomposition. The latter is not addressed here and will be the focus of future updates to the model.

## 2. Collatz et al. model

The equations and parameterizations of plant photosynthesis $A_n$ and stomatal conductance $g_s$ developed by Collatz et al. (1991) for $C_3$ plants and by Collatz et al. (1992) for $C_4$ plants are scaled up from leaf to canopy level in Sellers et al. (1996a). These equations have sound physiological bases and thorough descriptions to the interactive effects of environmental factors and stomatal control of plant photosynthesis and transpiration. In the leaf to canopy scaling-up strategy used in Sellers et al. (1996a), a plant canopy is simplified as a "big leaf". Fig. 1 is the schematic diagram showing the exchanges of sensible heat, latent heat and $CO_2$ between atmosphere and the canopy in Collatz et al. model (1991, 1992). The formations of Sellers et al. (1996a) can be summarized in the following five equations:

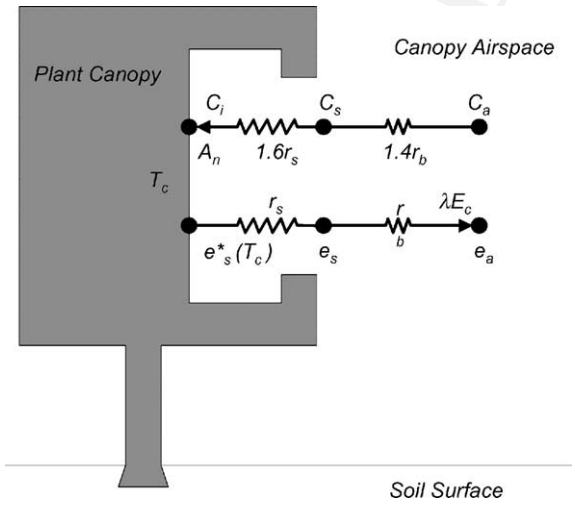


Fig. 1. Schematic diagram of Collatz' coupled photosynthesis-stomatal conductance model (canopy version in Sellers et al., 1996a). See Appendix A for symbol definition.

$$A_n = \frac{g_b}{1.4}\frac{C_a - C_s}{p} \quad (1)$$

$$A_n = \frac{g_s}{1.6}\frac{C_s - C_i}{p} \quad (2)$$

$$g_s = m\frac{pA_n e_s}{C_s e^*(T_c)} + bF \quad (3)$$

$$A_n = \min(W_c, W_e, W_s) - R_d \quad (4)$$

$$g_s(e^*(T_c) - e_s) = g_b(e_s - e_a) \quad (5)$$

The symbols in these equations are listed in Appendix A. Eq. (1) describes $CO_2$ transfer rate from canopy

airspace to leaf surface. Eq. (2) estimates $CO_2$ transfer rate from leaf surface to inside the stomata. Eq. (3) shows the relationship between stomatal conductance and photosynthesis at canopy scale based on Ball's (1988) stomatal conductance model. Eq. (4) is the leaf biochemical model that includes the leaf to canopy scaling approach of Sellers et al. (1992). Eq. (5) is the conservation equation for water transfer from inside stomata through stomata to the canopy airspace. The three limitations ($W_c$, $W_e$ and $W_s$) of photosynthetic rate in Eq. (4) are computed as follows for $C_3$ plants:

$$W_c = V_{max}\frac{C_i - \Gamma_*}{C_i + K_c(1 + O_i/K_o)}\Pi \quad (6)$$

$$W_e = \mathrm{PAR}(1-\omega_\Pi)\varepsilon_3\frac{C_i - \Gamma_*}{C_i + 2\Gamma_*}\Pi\left(\frac{\overline{G(\mu)}}{\mu}\right) \quad (7)$$

$$W_s = 0.5V_{max}\Pi \quad (8)$$

For $C_4$ plants, they are calculated with the following equations:

$$W_c = V_{max}\Pi \quad (9)$$

$$W_e = \mathrm{PAR}(1-\omega_\Pi)\varepsilon_4\Pi\left(\frac{\overline{G(\mu)}}{\mu}\right) \quad (10)$$

$$W_s = V_{max}2\times 10^4\frac{C_i}{p}\Pi \quad (11)$$

In these equations, the leaf to canopy scaling factor:

$$\Pi = \frac{VN(1-e^{-\bar{k}F/VN})}{\bar{k}} \quad (12)$$

The inputs needed by these equations include PAR, $T_a$, $T_c$, $e_a$, $C_a$ and $g_b$. The unknown variables are $A_n$, $g_s$, $C_i$, $C_s$ and $e_s$ (see Appendix A for symbol definitions).

## 3. Semi-analytical solution approach

Since Eqs. (1)–(5) are high-order non-linear functions, full analytical solutions cannot be obtained. Collatz et al. (1991, 1992) and Sellers et al. (1996a) use iterations to obtain numerical solutions. In this study, a semi-analytical solution procedure is developed. To simplify the solution, we first set the value of $e_s$ to be the average of $e_a$ and $e^*(T_c)$. Therefore, only Eqs. (1)–(4) are used to derive analytical solutions. We further rewrite Eq. (4) in a general form as follows:

$$A_n = A_1\frac{C_i - A_2}{A_3C_i + A_4} + A_5 \quad (13)$$

The expression for each $A_i$ ($i = 1, 2, 3, 4, 5$) for $C_3$ and $C_4$ plants is listed in Table 1.

If $A_1 \neq 0$ and $A_3 \neq 0$ in Eq. (13), a cubic equation of $C_i$ can be derived from Eqs. (1)–(3) and (13):

$$AC_i^3 + BC_i^2 + CC_i + D = 0 \quad (14)$$

If $A_1 \neq 0$ and $A_3 = 0$ in Eq. (13), a quadratic equation would be obtained:

$$a_cC_i^2 + b_cC_i + c_c = 0 \quad (15)$$

A detailed derivation and the definitions of the coefficients in Eqs. (14) and (15) are presented in Appendix B.

With the valid solution of $C_i$ obtained from the above procedure, we use Eq. (13) to computer $A_n$ if $A_3 \neq 0$. Otherwise,

$$A_n = A_1C_i + A_5 \quad (16)$$

From the value of $A_n$, we can inverse Eq. (1) to obtain the value of $C_s$ and finally the value of $g_s$ can be obtained from Eq. (3).

Fig. 2 is a flow chart of the above semi-analytical solution procedure. It starts from estimating the "leaf" surface water vapor pressure with the average of the canopy space water vapor pressure and the water vapor pressure insides the stomata. For any set of environmental conditions, the coefficients of Eq. (14) can be computed with the equations in Appendix B. Then an analytical solution of $C_i$ can be obtained by analytically solving the cubic equation. Once the value of $C_i$ corresponding to the set of the environmental conditions is obtained, the values of $A_n$, $g_s$, $C_s$ and a new $e_s$ can be obtained. The new $e_s$ value is normally very close to its previous value. If not, the coefficients of Eq. (14) can be re-computed with the new $e_s$ value and the steps to solve the cubic equation and to compute the values of $A_n$, $g_s$, $C_s$ and $e_s$ will be repeated. This procedure has two important aspects: (1) with the analytic approach, the physically and biologically unrealistic solutions are avoided. Under any specific environmental conditions, whether reasonable solutions of the model can be obtained depends on whether the

Table 1
Expressions of the variables $A_i$ ($i = 1, 2, 3, 4, 5$) in Eq. (13)

| Plant type | Photosynthetic limitation | $A_1$ | $A_2$ | $A_3$ | $A_4$ | $A_5$ |
|---|---|---|---|---|---|---|
| $C_3$ | $W_c$ | $V_{max}\Pi$ | $\Gamma_*$ | 1 | $K_c(1+O_i/K_o)$ | $-R_d$ |
| | $W_e$ | $PAR(1-\omega_\Pi)\varepsilon_3\Pi(\overline{G(\mu)}/\mu$ | $\Gamma_*$ | 1 | $2\Gamma_*$ | $-R_d$ |
| | $W_s$ | $0.5V_{max}\Pi$ | 0 | 1 | 0 | $-R_d$ |
| $C_4$ | $W_c$ | $V_{max}\Pi$ | 0 | 1 | 0 | $-R_d$ |
| | $W_e$ | $PAR(1-\omega_\Pi)\varepsilon_4\Pi(\overline{G(\mu)}/\mu$ | 0 | 1 | 0 | $-R_d$ |
| | $W_s$ | $2\times10^4(V_{max}/p)\Pi$ | 0 | 0 | 1 | $-R_d$ |

cubic equation of $C_i$ has a realistic solution. We have tested the above method under a range of environmental conditions, and have not found any case with no valid solution. (2) The initial value of $e_s$ is very close to its solution when wind speed is not very large which is true for most leaves within a canopy, so that excluding $e_s$ in the analytical solution procedure makes the derivation simple. Although we list iteration for $e_s$ in Fig. 2, in most cases, no iteration is needed when the initial conditions of $e_s$ are selected as described above.

Fig. 3 demonstrates the results from the above semi-analytical solution method compared with the results from the iterative numerical solution method for a set of typical environmental conditions listed in Table 2. Sensitive parameters are also listed in Table 2. Other parameter values are adopted from Sellers et al. (1996a). The results are almost identical in most cases except that the numerical solution method may become unstable when the value of PAR becomes higher than 400 ($W\,m^{-2}$). This confirms the potential instability problem in iterations as claimed in Baldocchi (1994).

Table 2
The typical environmental conditions and model parameters for the plots in Fig. 3

| | |
|---|---|
| Canopy leaf area index LAI | 3.0 |
| Above canopy $CO_2$ concentration $C_a$ | 34 Pa |
| Above canopy air temperature $T_a$ | 25 °C |
| Above canopy vapor pressure $e_a$ | 2000 Pa |
| "Leaf" boundary layer resistance $r_b$ | 50 $s\,m^{-1}$ |
| Rubisco maximum catalytic capacity $V_{max}$ | 60 $\mu mol\,m^{-2}\,s^{-1}$ |
| PAR extinction coefficient $\kappa$ | 0.45 |
| Time-mean projection of leaves $[G(\mu)/\mu]$ | 1.0 |
| Photosynthesis optimal temperature top | 30 °C |
| Photosynthesis minimum temperature $T_{low}$ | 15 °C |
| Photosynthesis maximum temperature $T_{high}$ | 45 °C |

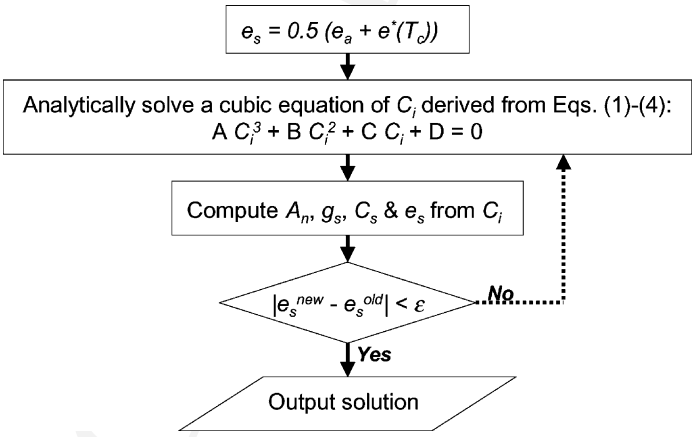


Fig. 2. The semi-analytical solution procedure for the Collatz et al. $A_n$–$r_s$ coupled model.

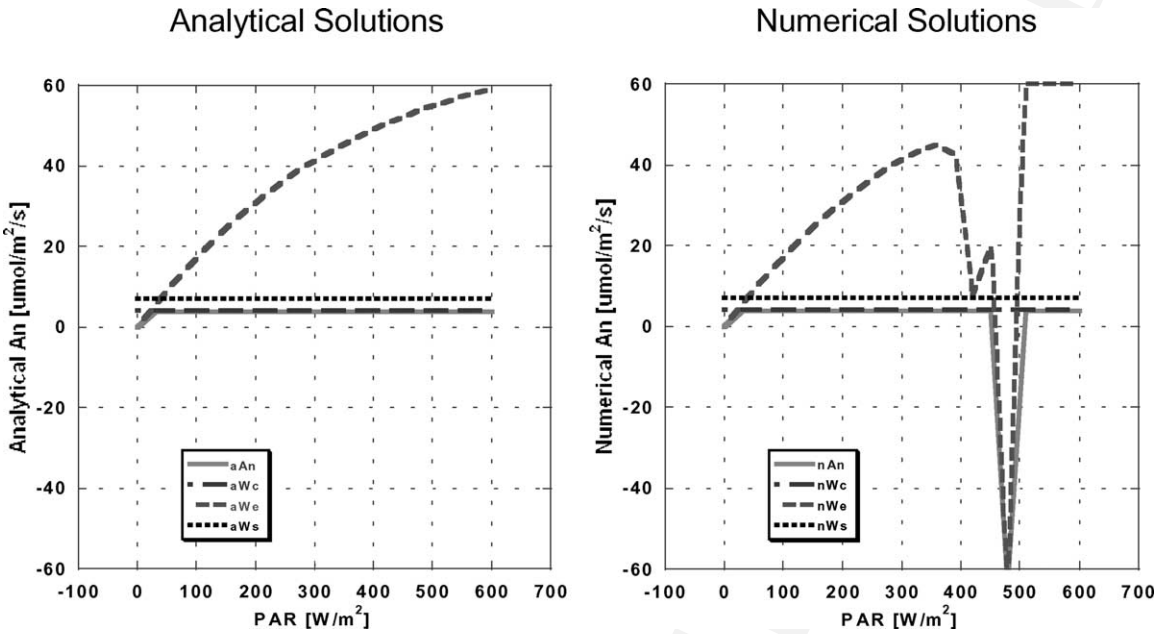


Fig. 3. Comparison between the analytical and numerical solution methods for the Collatz et al. $A_n$–$r_s$ coupled model. The symbols a$A_n$, a$W_c$, a$W_e$, a$W_s$ represent results from the analytical solution approach. The symbols n$A_n$, n$W_c$, n$W_e$, n$W_s$ are the results from the numerical iteration method.

## 4. Implementing Collatz et al. model in the simplified biosphere model (SSiB)

Stomatas on plant leaves control both water vapor transfer from inside to outside and $CO_2$ transfer from outside to inside as indicated in Fig. 1. The original SSiB model (Xue et al., 1996a,b) simulates only the water vapor transfer by using the Jarvis' empirical approach (Jarvis, 1976) to compute the stomatal resistance $r_c$ to water vapor transfer. With the reasons stated previously, we enhance the SSiB model with the $CO_2$ simulation capability by replacing the submodel of stomatal resistance in the original SSiB with the Collatz et al. model introduced in the previous sections.

To compute the canopy resistance (the inverse of canopy stomatal conductance) with the photosynthesis-stomatal conductance model (Eqs. (1)–(5)), one needs to know the canopy airspace $CO_2$ concentration $C_a$. The value of $C_a$ needs to be specified first, which is the product of the balance of $CO_2$ fluxes into and out of the canopy airspace. For a typical day-time, the influxes include the $CO_2$ transfer from the atmosphere and from the soil surface into the canopy airspace, namely $F_{ca}$ and $F_{cs}$. The sink of the canopy airspace $CO_2$ is the canopy photosynthesis $A_n$. If $F_{cs}$ and the $CO_2$ concentration of the atmosphere above the canopy, $C_m$, are known, then we have

$$C_a = C_m - pr_a(A_n - F_{cs}) \quad (17)$$

because

$$F_{ca} = \frac{C_m - C_a}{pr_a} = A_n - F_{cs}. \quad (18)$$

Eq. (18) can be used to simulate the $CO_2$ flux above a plant canopy. The soil respiration term $F_{cs}$ in the above equations will be the focus of future updates of the model. In this paper, it is setup to be a constant (e.g. $F_{cs} = 4.0\,\mu mol\,m^{-2}\,s^{-1}$ for the Manaus data set described in Section 6.2).

Soil moisture is an important factor influencing the carbon flux. In SSiB, the equation of the adjustment factor $f(\psi)$ of the stomatal conductance $g_s$ for soil moisture limitation is

$$f(\psi) = 1 - \exp\{-C_2[C_1 - \ln(-\psi)]\} \quad (19)$$

where $\psi$ is the soil water potential. $C_2$ depends on the vegetation type, and $C_1$ is a constant obtained using the wilting point. The stomates completely close at the wilting point in the model. $C_2$ is a slope factor. A large $C_2$ means that the $f(\psi)$ changes from 0 to 1 very fast when soil water content varies from wilting point to the point stomates start to close. This approach differs from that of Sellers et al. (1996a,b) who apply water stress scaling to the maximum photosynthetic capacity ($V_{max}$) rather than the stomatal conductance directly. Note that in Table 1 of Xue et al. (1991) the values of $C_1$ and $C_2$ should be interchanged.

## 5. Scaling up the Collatz et al. model from leaf to canopy

Fig. 3 indicates that canopy net photosynthesis rate gets saturated when photosynthetically active radiation PAR is greater than about 50 (W m$^{-2}$). According to field measurements introduced in Section 6 and documentations in the literature (e.g. Thornley and Johnson, 1990), this saturation PAR level for most leaves is greater than 200 (W m$^{-2}$). One of the causes may be that implementation of the Collatz et al. model in the SSiB_2 model (Sellers et al., 1996a,b) assumes equal acceptance of PAR by all leaves within a canopy when the equations are integrated for all leaves in the canopy. In reality, only sunlit leaves in plant canopy receive direct PAR while shaded leaves receive diffusive PAR only. To consider this fact, we implement the Collatz et al. model for sunlit leaves and shaded leaves separately while the equation set (Eqs. (1)–(12)) and the analytical solution approach introduced previously are kept the same.

Instead of using the total PAR for the Collatz et al. model, we separate PAR to direct radiation $\mathrm{PAR_{dr}}$ and diffusive radiation $\mathrm{PAR_{df}}$. According to Norman (1982), if the PAR measurement above the canopy is $\mathrm{PAR_0}$ and the fraction of diffusive PAR is $f_d$, then

$$\mathrm{PAR_{df}} = f_d \mathrm{PAR_0} \exp(-0.5F^{0.7}) + 0.07(1-f_d)\mathrm{PAR_0}(1.1-0.1F)\mathrm{e}^{-\sin\theta_s} \quad (20)$$

$$\mathrm{PAR_{dr}} = \frac{(1-f_d)\mathrm{PAR_0}\cos\theta_{ls}}{\sin\theta_s} \quad (21)$$

where $\theta_s$ is elevation angle of the sun and calculated from the time of day, the day of year and the latitude of observational site with the equation used in Campbell (1977, p. 55). The $\theta_{ls}$ is the mean angle between the leaf normal and the sunlight. We select $\theta_{ls} = 60^\circ$ for a canopy with spherical leaf angle distribution (Norman, 1982). Accordingly, the PAR received by the sunlit leaves $\mathrm{PAR_{slt}} = \mathrm{PAR_{dr}} = \mathrm{PAR_{df}}$ while the PAR received by the shaded leaves $\mathrm{PAR_{shd}} = \mathrm{PAR_{df}}$.

Assuming random leaf positioning and spherical leaf angle distribution, the sunlit leaf area index $F_{slt}$ as

$$F_{slt} = 2[1-\exp(-0.5F/\sin\theta_s)]\sin\theta_s \quad (22)$$

the shaded leaf area index $F_{shd} = F - F_{slt}$.

Using $\mathrm{PAR_{slt}}$ to run the analytical solution procedure for the Collatz et al. model introduced previously for a unit sunlit leaf (leaf area index = 1.0), one obtains the net photosynthesis rate $A_{n\,slt}$ and stomatal conductance $g_{slt}$. Similarly using $\mathrm{PAR_{shd}}$ for a unit shaded leaf, one obtains $A_{n\,shd}$ and $g_{shd}$. The canopy total net photosynthetic rate $A_n$ and stomatal conductance are then computed as

$$A_n = A_{n\,slt}F_{slt} + A_{n\,shd}F_{shd} \quad (23)$$

$$g_c = \frac{1}{(F_{slt}/g_{slt}) + (F_{shd}/g_{shd})} \quad (24)$$

By this point, we have introduced three different versions of implementing the Collatz et al. model of plant photosynthesis and stomatal conductance: (1) the original implementation in SSiB_2 using iteration solution method; (2) a modified version using analytical solution method; and (3) another modified version using both the analytical solution method and the sunlit–shaded leaf separation scaling method. For this study of enhancing the SSiB for carbon simulation, we use field measurements to evaluate the following three versions of SSiB: (1) the original SSiB model using Jarvis' stomatal model (for convenience we will refer this version as SSiB_0); (2) the SSiB model using the Collatz et al. model in Sellers et al. (1996a) modified with the analytical solution method (referred to as SSiB_1); and (3) the SSiB model using the Collatz et al. model modified with the analytical solution method and the sunlit–shaded leaf separation scaling method (referred to as SSiB_2).

## 6. Field measurement data sets for model evaluation

Three data sets from two field experiments are used to evaluate the enhanced SSiB model. The two field experiments are the ABRACOS field experiment and the Manaus Eddy Covariance Study.

### 6.1. ABRACOS field experiment (1990 and 1991)

The ABRACOS is a comprehensive observational study of land surface–atmosphere interactions in large-scale clearings caused by tropical deforestation (Shuttleworth et al., 1991). The main objective of ABRACOS was to provide comparative data from adjacent forested and cleared areas, and to provide representative parameters and data from clearings for GCM studies. The data used in this study were collected during the first two experimental seasons of ABRACOS at the Fazenda Dimona ranch site (02°19′S, 60°19′W), 100 km north of Manaus in central Amazonia. Mission 1 was conducted from 4 October to 2 November 1990 and Mission 2 was conducted from 29 June to 10 September 1991. Vegetation at the experiment site is mainly $C_4$ grass. Further details of the ranch and the experimental site are described by Wright et al. (1992), McWilliams et al. (1993), and Bastable et al. (1993).

The ABRACOS Mission 1 (M1) and Mission 2 (M2) data sets include incoming and reflected radiation of wavelength 0.3–3.0 μm, global radiation, soil heat flux, ambient air and wet-bulb temperatures, soil temperature, precipitation, and wind speed and direction. Manufacturer supplied calibrations were used for all the radiation instruments. The thermometers were calibrated against a standard and are accurate to within ±0.1 K. The data were recorded using solid state recorder, which sampled every 10 s.

Three measurement systems, including a Campbell Scientific Ltd. (UK) Bowen-ratio system, the Mk 2 'Hydra' Eddy correlation device, and a logarithmic wind and scalar profile measurement rig were used to estimate fluxes of water vapor and sensible heat. There was excellent agreement between the three measurement systems, the data from which were combined to form a complete hourly time series record for each experimental period. No $CO_2$ fluxes were measured during ABRACOS. Therefore, this data set is used to evaluate the model simulations of the water and energy budgets after introducing a complex photosynthesis process, and to compare the model simulations with two different stomatal conductance parameterizations.

### 6.2. Manaus Eddy Covariance Study (1996)

Another data set used for this paper was obtained from an Eddy Covariance Study which was conducted from 6 July 1995 to 24 August 1996 in the Reserva Biologica do Cuieiras (2°35′22″S, 60°6′55″W), some 60 km north of Manaus (Malhi et al., 1998). This is part of a very extensive, continuous area of dense lowland terra firm tropical rain forest. Vegetation of the site is very similar to the site studied by Fan et al. (1995). One of the primary focuses in the measurement is to examine and describe the nature and magnitude of the diurnal $CO_2$ flux and its relationship to meteorological conditions (Williams et al., 1998). The fluxes were measured in an Edisol Eddy covariance system (Malhi et al., 1998). Meteorological data were collected with an automatic weather station. The gas analyzers were calibrated at least weekly using zero and fixed concentration $CO_2$ and water vapor samples. Very little drift in analyzer concentration was noted over a diurnal cycle or on a week-to-week basis. Real time data were collected as 10 min average. Corrections were applied for the dampening of fluctuations at high frequencies using the approach outlined by Moore (1986) and Moncrieff et al. (1997). For the study in this paper, the data collected only from late December 1995 to mid-January, 1996 were used because of the better continuity and certainty of biophysical parameters. For convenience, this data set is called "Manaus data".

## 7. Results and discussion

The SSiB model will be used to study the impact of land cover change in Amazonia region on the regional climate and carbon balance using the Collatz et al. photosynthesis and stomatal conductance model. Thus, proper simulations in both carbon flux and heat fluxes are necessary. The original SSiB model using the empirical Jarvis stomatal model (SSiB_0) has produced reasonable simulations of heat fluxes in the

off-line tests for Amazon sites (e.g. Xue et al., 1991, 1996a). As the first step, we must check whether the more realistic but more complex approach for simulation of stomatal control is still able to yield reasonable simulations in heat fluxes. Then we will evaluate how the two modified SSiB versions (SSiB_1 and SSiB_2) perform for the $CO_2$ flux simulations.

### 7.1. Simulation of heat fluxes (SSiB_0, SSiB_1 and SSiB_2 versus observations)

In the off-line numerical experiments, we used observed temperature, humidity, and wind speed at the reference height, precipitation and net radiation at the surface as forcing to test SSiB. SSiB calculates energy components, including the latent heat, sensible heat, and ground heat fluxes, momentum flux, canopy photosynthesis, and upward short wave and long wave radiation. All of these components, except long wave radiation, were measured during ABRACOS field experiments. The values of vegetation parameters used for this off-line validation were from measurements in the ABRACOS field campaign and are listed in Table 3.

ABRACOS intensive flux observations were made for a continuous 30-day period during Mission 1 (M1) and for 74 days during Mission 2 (M2). Figs. 4 and 5 are the comparisons between the observed and simulated daily means of latent heat, sensible heat and soil heat fluxes for three versions of the SSiB model (SSiB_0, SSiB_1 and SSiB_2). The correlation coefficients of the daily mean fluxes for the entire periods of both M1 and M2 are listed in Table 4. The three versions of SSiB produce very similar simulations for the three fluxes. Fig. 5a shows that in M2 the simulated latent heat flux closely follows observations. The observed latent heat fluxes dropped sharply several times during M2 (3, 4, and 25 August and 2 September). The model simulated these dramatic changes and recovered very well. In M1, although the three versions of the model generally followed the trend, the simulations of the three heat fluxes fluctuated about the observations (Fig. 4). In the early October, the models underestimated latent heat flux and overestimated sensible heat flux by about 30%. But in the middle October, the model overestimated latent heat flux and underestimated sensible heat flux by about 20%. These fluctuations might result from the biases of soil heat flux simulations from their observations (Fig. 4c). In general, the simulations of the heat fluxes from the two modified SSiB versions (SSiB_1 and SSiB_2) are very similar to those from the original SSiB (SSiB_0).

For the Manus data set, detailed soil and vegetation information was not available except that the vegetation cover of the study site is a continuous area of dense lowland terra firm tropical rainforest and that the leaf area index was 5–6 and canopy height 30 m according to Malhi et al. (1998). In an off-line test, it is important to have a proper set of vegetation and

Table 3
Vegetation parameters of the ABRACOS data set

| Vegetation parameters | Values |
|---|---|
| Surface albedo | 0.18 |
| Leaf area index (LAI) | 1 (M1), 2 (M2) |
| Greenness | 0.7 (M1), 0.9 (M2) |
| Vegetation cover fraction | 0.85 |
| Soil layer thicknesses (m) | 0.02, 0.98, 1 |
| Soil hydraulic conductivity at saturation ($ms^{-1}$) | $2.2e^{-5}$ |
| Sorption parameter, $B$ | 6.9 |
| Soil water potential at saturation (m) | −0.035 |
| Porosity | 0.59 |
| Minimum stomatal resistance ($sm^{-1}$) | 140 |
| Adjustment factor for water vapor deficit | 0.020 |
| Adjustment factor for temperature | 295, 276, 323 |
| Adjustment factor for soil moisture | 1.73, 5.8 |
| Rooting depth (m) | 1.0 |
| Surface roughness length (m) | 0.026 |
| Displacement height (m) | 0.18 |
| Vegetation height (m) | 0.28 |

Table 4
Correlation coefficients between the hourly output of heat fluxes from the three model versions and the field observations

| Flux | Model | ABRACOS Mission 1 (M1) | ABRACOS Mission 2 (M2) | Manaus |
|---|---|---|---|---|
| *H* | SSiB_0 | 0.87 | 0.91 | 0.86 |
| | SSiB_1 | 0.88 | 0.90 | 0.91 |
| | SSiB_2 | 0.88 | 0.89 | 0.91 |
| LE | SSiB_0 | 0.94 | 0.96 | 0.96 |
| | SSiB_1 | 0.94 | 0.97 | 0.97 |
| | SSiB_2 | 0.94 | 0.95 | 0.98 |
| *G* | SSiB_0 | 0.83 | 0.91 | 0.91 |
| | SSiB_1 | 0.82 | 0.90 | 0.73 |
| | SSiB_2 | 0.82 | 0.83 | 0.84 |

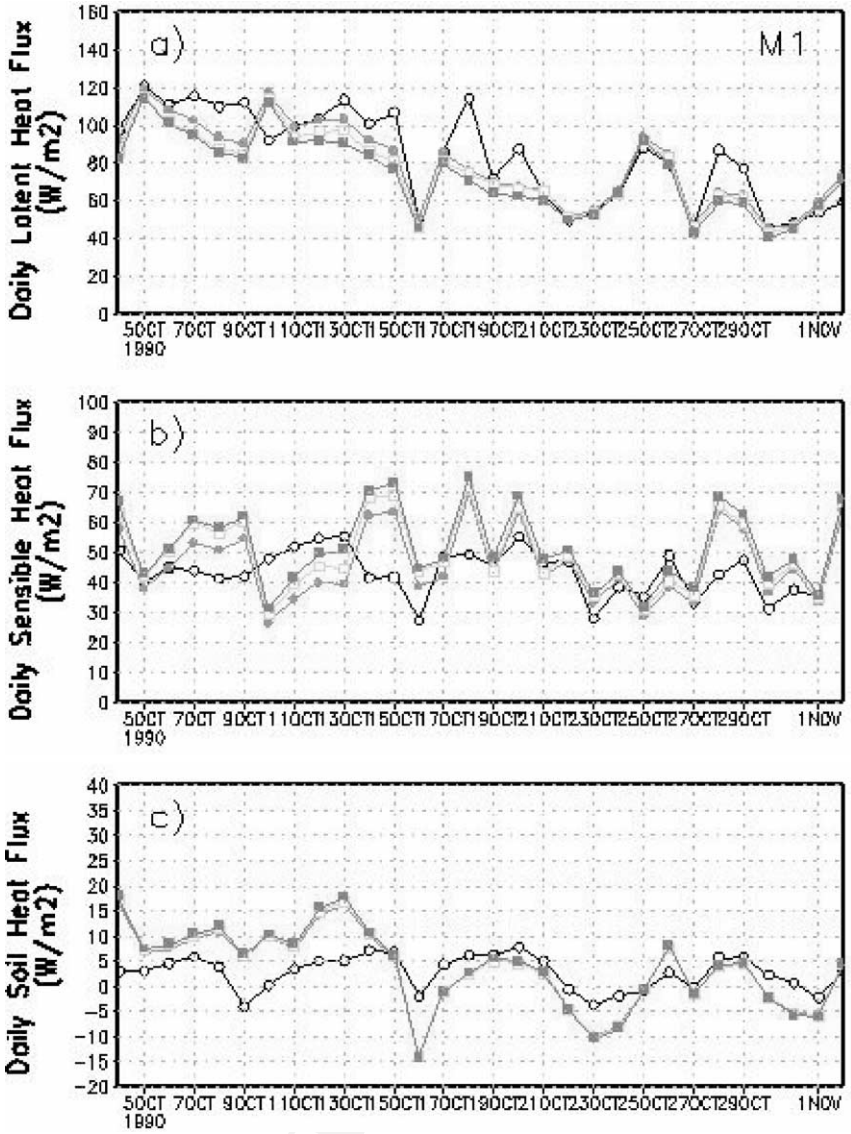


Fig. 4. The daily mean values of (a) latent heat flux, (b) sensible heat flux, and (c) soil heat flux obtained from the observations during the Mission 1 of the ABRACOS field experiment (line marked with open circles), the simulations of SSiB_0 (solid squares), the simulations of SSiB_1 (solid circles) and the simulations of SSiB_2 (open squares). If solid circles or open squares are not seen, they are overlaid by solid squares.

soil parameters and it may cause systematic errors if these parameters are not setup correctly (Xue et al., 1996b; Xue et al., 1997). Because we have no measured surface vegetation and soil information, we use the vegetation and soil parameters from a vegetation and soil parameter table, which is used in the coupled atmospheric/SSiB model (e.g. Xue et al., 2001). In this study, we base on the above-mentioned vegetation type information to specify the land parameter values. Fig. 6 shows the result from three versions of SSiB. It is evident that all three versions are able to simulate the variability in latent heat, sensible heat

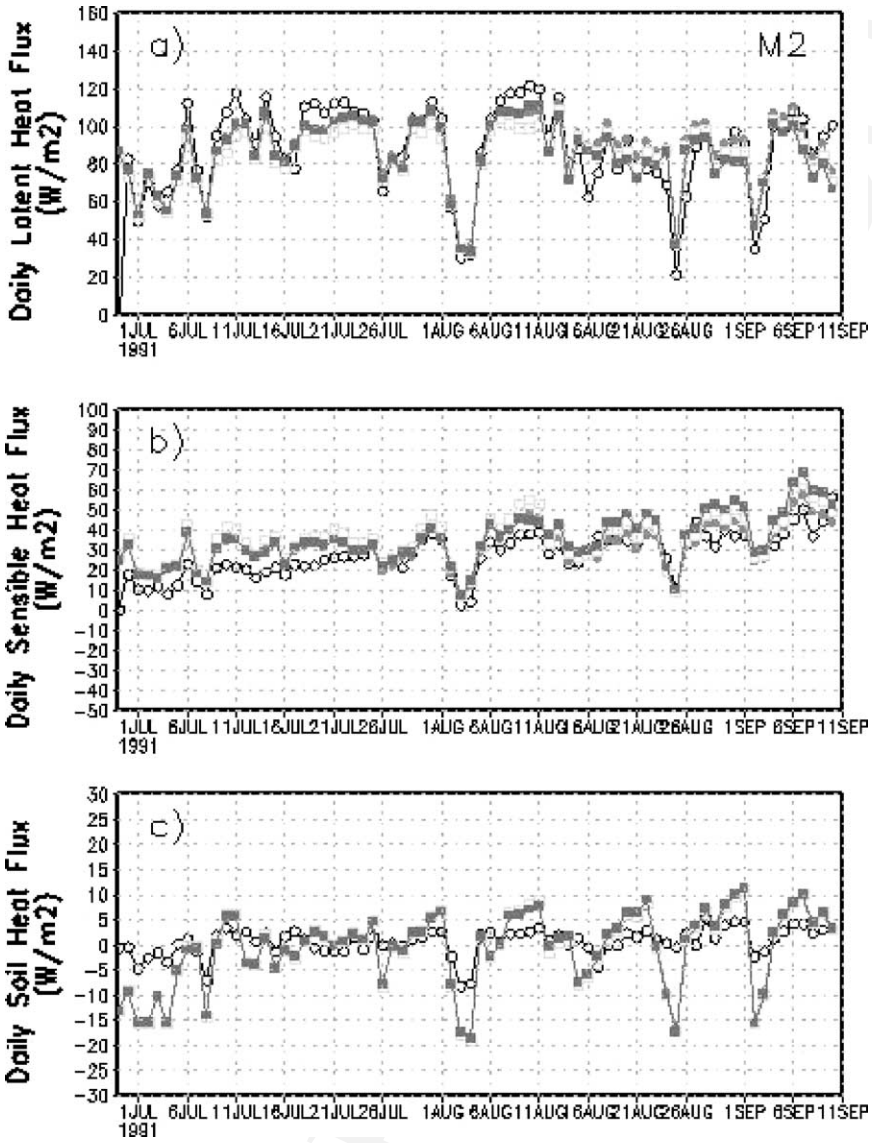


Fig. 5. The daily mean values of (a) latent heat flux, (b) sensible heat flux, and (c) soil heat flux obtained from the observations during the Mission 2 of the ABRACOS field experiment (line marked with open circles), the simulations of SSiB_0 (solid squares), the simulations of SSiB_1 (solid circles) and the simulations of SSiB_2 (open squares). If solid circles or open squares are not seen, they are overlaid by solid squares.

and soil heat fluxes well. The correlations between the model outputs and the field observations are similar to the results for the ABROCOS data sets (Table 4). This result further indicates that the two modified versions of SSiB do not compromise the capability of the original SSiB in simulating the latent heat, sensible heat and soil heat fluxes.

### *7.2. Simulations of $CO_2$ flux (SSiB_1 and SSiB_2 versus observations)*

The primary goal of this work is to enhance the SSiB model with $CO_2$ flux simulation capability. How the two modified versions of the SSiB model perform in $CO_2$ flux simulation is of the most concern.

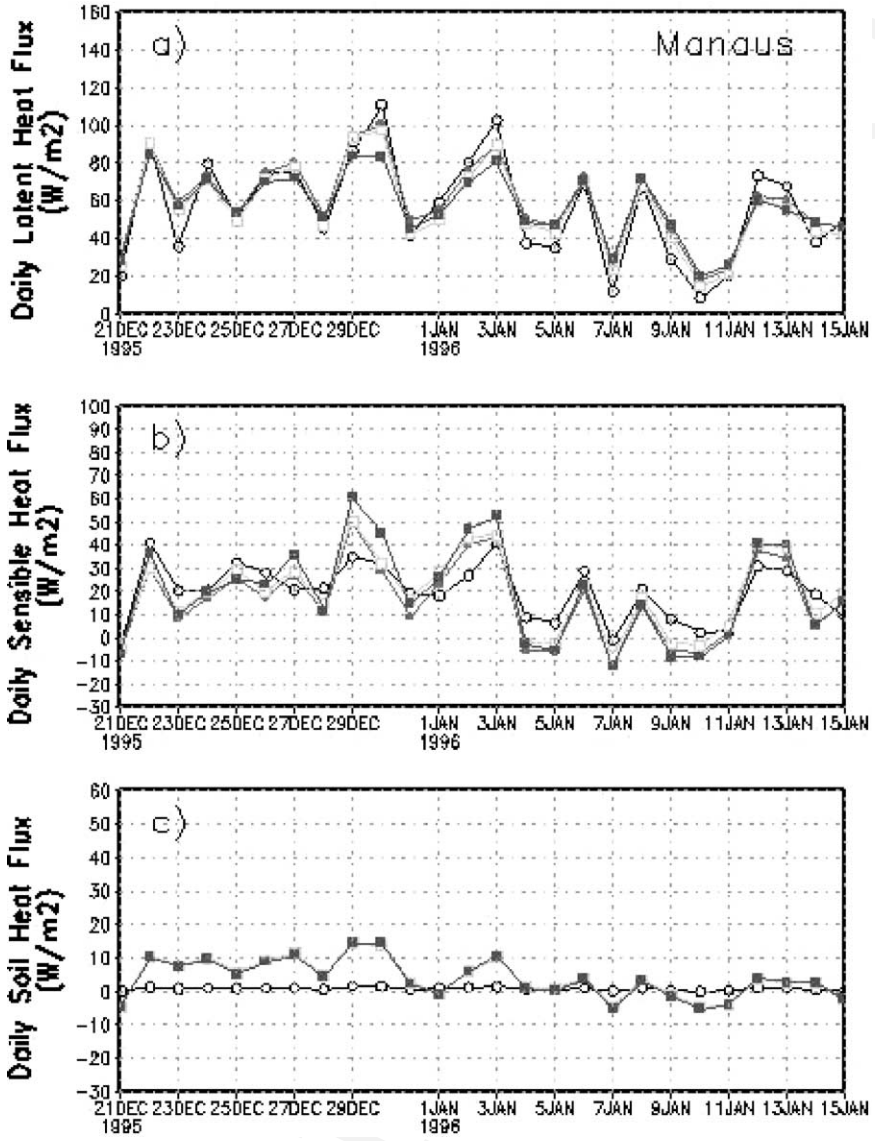


Fig. 6. The daily mean values of (a) latent heat flux, (b) sensible heat flux, and (c) soil heat flux obtained from the observations during the Eddy Covariance Study (line marked with open circles), the simulations of SSiB_0 (solid squares), the simulations of SSiB_1 (solid circles) and the simulations of SSiB_2 (open squares). If solid circles or open squares are not seen, they are overlaid by solid squares.

Using the only $CO_2$ flux measurements in the Manaus data set, we can find the answer to this question from the results demonstrated in the following figures.

Fig. 7 is a comparison between the simulations (marked with solid) circles) by (a) SSiB_1 or (b) SSiB_2 and their corresponding observations (open circles) of the above canopy hourly $CO_2$ flux for the 26 days in the Manaus data set. The correlation coefficient between the hourly simulation and field observation is 0.73 for SSiB_1 and 0.84 for SSiB_2. Although both SSiB_1 and SSiB_2 simulated the diurnal cycles of the $CO_2$ flux, the simulations by SSiB_1, which uses the same leaf to canopy scaling

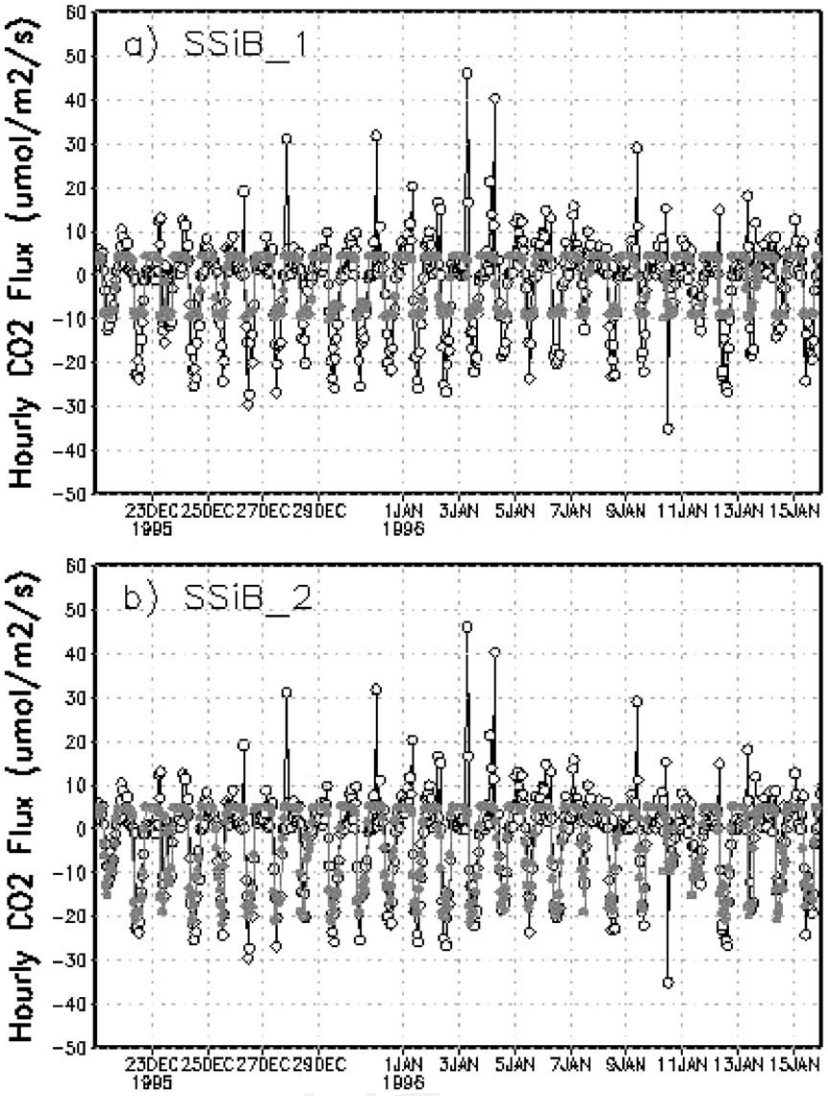


Fig. 7. The hourly above canopy $CO_2$ flux simulations (solid circles) and their field observations (open circles) for the 26-day data set from the Manaus Eddy Covariance Study: (a) for SSiB_1; (b) for SSiB_2. Negative value means that $CO_2$ is transported from the above canopy atmosphere downward to the canopy.

strategy as in SSiB_2 (Sellers et al., 1996a), have very similar maximums during midday for all 26 days. The simulations by SSiB_2, which computes net photosynthetic rate and stomatal conductance for sunlit and shaded leaves, respectively, have diurnal cycles varying mainly with incoming photosynthetically active radiation. The observed diurnal cycles of $CO_2$ flux follow the PAR diurnal pattern. Thus, the SSiB_2 simulations have a higher correlation coefficient (0.84).

Fig. 8 is the diurnal cycles of the model simulations plotted against the field observations averaged over the 26 days. Despite general consistency of the simulations of both SSiB_1 and SSiB_2 with observations, a noontime square wave in the simulations of SSiB_1 is evident. To more clearly examine the difference in

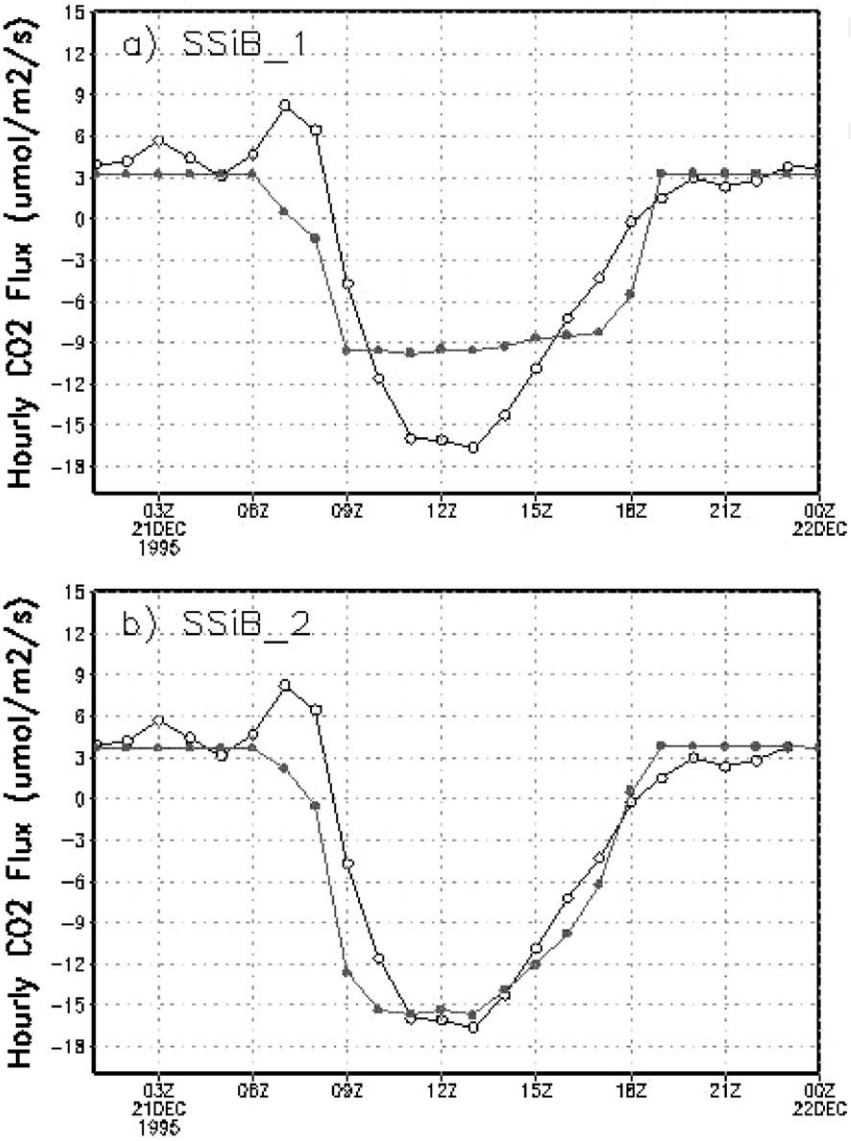


Fig. 8. The averaged diurnal curve of the above canopy $CO_2$ flux simulations (solid circles) and their field observations (open circles) for the 26-day data set from the Manaus Eddy Covariance Study: (a) for SSiB_1; (b) SSiB_2. Negative value means that $CO_2$ is transported from the above canopy atmosphere downward to the canopy.

the $CO_2$ flux diurnal cycle simulations by SSiB_1 and SSiB_2, the simulated plant photosynthetic rate $A_n$ and their three limitations (namely, the RuBP saturation limited rate $W_c$, the electron transportation limited rate $W_e$, and the sink limited rate $W_s$) averaged over the 26 days are plotted in Fig. 9 for SSiB_1 and Fig. 10 for SSiB_2. As in Eq. (4), the photosynthetic rate $A_n$ is the minimum of these three limitations adjusted with a quadratic equation (Collatz et al., 1991). Thus, the curve of net photosynthetic rate $A_n$ in Fig. 9 goes beneath the lowest of $W_c$, $W_e$ and $W_s$. For most of the day-time, $W_c$ simulated by SSiB_1 is the lowest and does not change much for more than 6 h around noontime. Thus, the net photosynthetic rate $A_n$ follows

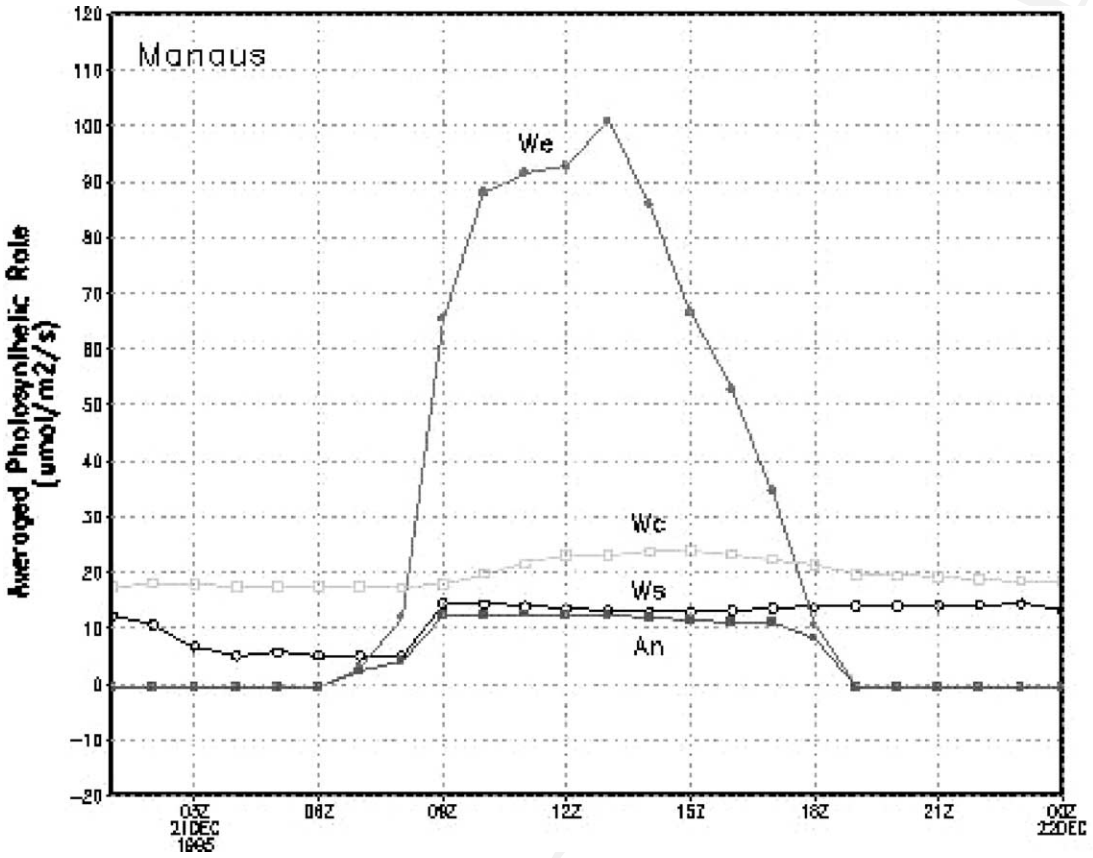


Fig. 9. The averaged diurnal curve of the canopy $CO_2$ photosynthetic rate and its three components simulated by Phost_1. Canopy net photosynthesis rate $A_n$ is marked with solid squares. The Rubisco limitation $W_c$ is open circles. The PAR limitation $W_e$ is solid circles. The sink limitation $W_s$ is open squares.

$W_c$ and shows a day-time square wave. This day-time square wave is not consistent with observations well documented in the literature (Thornley and Johnson, 1990). One of the reasons for this incorrect simulation by SSiB_1 in Fig. 9 may be that the parameters of the Collatz et al. model were setup incorrectly so that the simulations of $W_e$ are too large or the computed values of $W_c$ or $W_s$ are too small. However, as stated in Section 5, an apparent reason for the incorrect simulation of SSiB_1 is the strategy of scaling the Collatz et al. model from leaf to canopy in Sellers et al. (1996a). The scaling-up method treats all leaves within the plant canopy the same way. This may have underestimated the light saturation phenomenon of plant leaves (Chen et al., 1999). This underestimation of light situation may have caused the simulation of $W_e$ being too high. SSiB_2 attempts to avoid this problem by implementing the Collatz et al. model to sunlit leaves and shaded leaves separately. The results shown in Figs. 7b and 8b from SSiB_2 demonstrated significant improvement.

Fig. 10 plots the daily above canopy $CO_2$ flux averages of the model simulations and their field observations. For SSiB_1, because of the unrealistic square wave in the diurnal variation of plant photosynthetic rate, the simulated daily above canopy $CO_2$ flux averages (solid circles) do not match the observations well (open circles). For SSiB_2, its simulations (open squares) improve obviously over the simulation by SSiB_1. The correlation coefficient between the averages of the simulated daily above canopy $CO_2$ flux and their corresponding observations is only 0.42 for

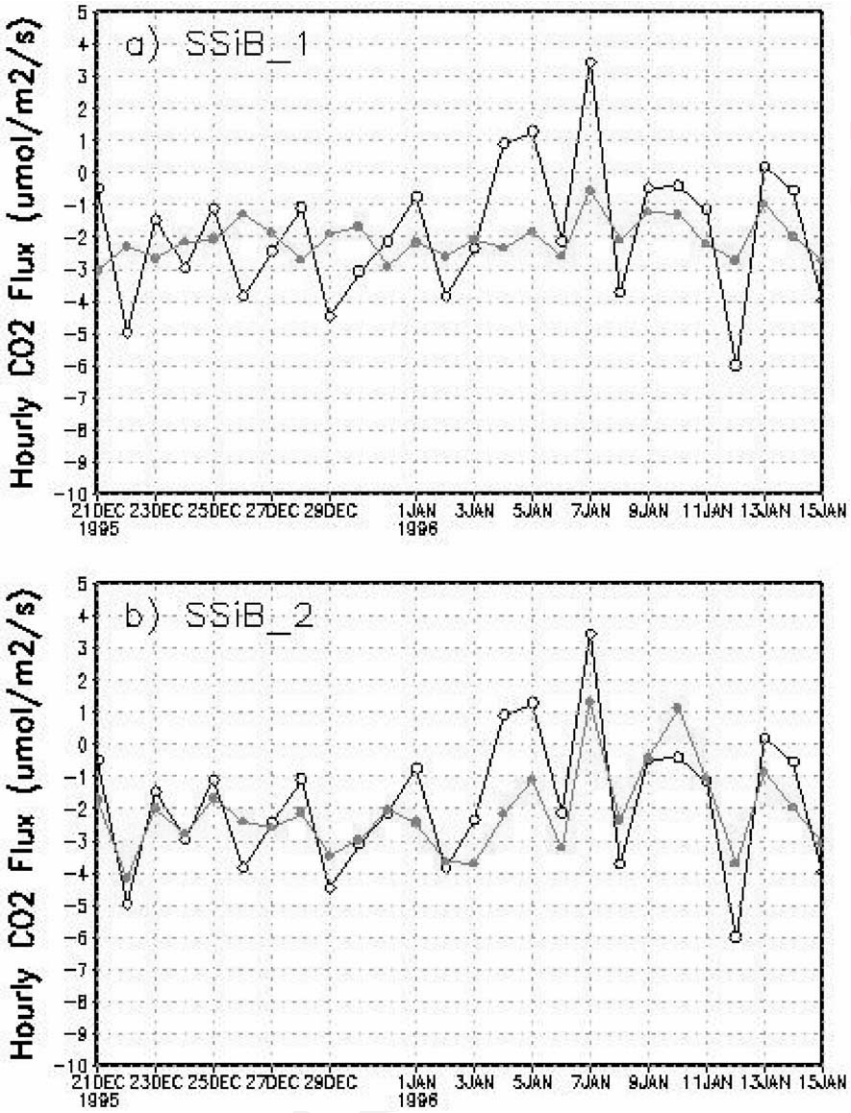


Fig. 10. The daily means of the above canopy $CO_2$ flux simulations (solid circles) and their field observations (open circles) for the 26-day data set from the Manaus Eddy Covariance Study: (a) for SSiB_1; (b) for SSiB_2. Negative value means that $CO_2$ is transported from the above canopy atmosphere downward to the canopy.

SSiB_1 and 0.80 for SSiB_2. In this paper, we set the soil respiration rate as a constant. It will be the focus of further studies to improve the capability of the SSiB model in $CO_2$ flux simulations. With a more realistic simulation of $F_{cs}$ in Eq. (18), the simulation result of $F_{ca}$ by SSiB_2 is expected to be even better.

## 8. Conclusions

Using three data sets collected from two large-scale field experiments, this study aims to improve the solution method and scaling-up approach of the Collatz et al. model of plant photosynthesis and stomatal conductance in order to implement the model in the SSiB

for $CO_2$ flux simulations. From the results obtained we can make the following conclusions:

(1) The Collatz et al. model of plant photosynthesis and stomatal conductance can solved with a semi-analytic method, which brings with better computational efficiency and stability for the coupled land surface–atmosphere interaction models.
(2) Implementation of the analytic solution approach for $CO_2$ flux solution in the SSiB model produces reasonable simulations of latent heat, sensible heat and soil heat fluxes and enhances the SSiB into a new generation model.
(3) The leaf to canopy scaling-up strategy used in Sellers et al. (1996a) for the implementation of the Collatz et al. model results in a day-time square wave in the net photosynthetic rate simulations. Considering the sunlit leaves and shaded leaves separately in the Collatz et al. model implementation in the SSiB model improves the photosynthesis and $CO_2$ flux simulations significantly.

## Acknowledgements

The authors would like to thank Dr. John Grace, Dr. Yadvinder Malhi of University of Edinburgh in United Kingdom and Dr. Antonio D. Nobre of Centro de Previsao de Tempo e Estudos Climaticos, Brazil, for providing field observation data of the Manaus Eddy Covariance study. Drs. J. Gash and H. G. Basetable of the Institute of Hydrology (UK) and their Brazilian collaborators are thanked for compiling and providing the ABRACOS data. This study was supported by NASA's grant of the LBA-Hydrometeorology program (NASA Grant NAG59386). The authors would also like to thank the anonymous reviewers and the editor for their constructive comments and recommendations.

## Appendix A. List of symbols with units and definition

| Symbol | Units | Definition |
|---|---|---|
| $A_n$ | $\mu mol\, m^{-2}\, s^{-1}$ | Net $CO_2$ assimilation of the canopy |
| $A$, $A_i$ $(i = 1, \ldots, 7)$, $a_c$ | | Interim variables for the analytic solutions |
| $B$, $B_1$, $B_2$, $b_c$ | | Interim variables for the analytic solutions |
| $b$ | $\mu mol\, m^{-2}\, s^{-1}$ | Coefficient in Eq. (3) (0.01 for $C_3$, 0.04 for $C_4$ vegetation) |
| $C$, $c_c$ | | Interim variables for the analytic solutions |
| $C_a$ | Pa | $CO_2$ concentration of the atmosphere |
| $C_i$ | Pa | $CO_2$ concentration inside plant leaves |
| $C_s$ | Pa | $CO_2$ concentration at leaf surface |
| $C_1$, $C_2$ | | Empirical coefficients of soil moisture adjustment factor, Eq. (19) |
| $e_a$ | Pa | Water vapor pressure at the reference height |
| $e^*(T)$ | Pa | Saturation vapor pressure at temperature $T$ |
| $e_s$ | Pa | Water vapor pressure at leaf surface |
| $\varepsilon_3/\varepsilon_4$ | $mol\, mol^{-1}$ | Intrinsic quantum efficiency of leaf photosynthesis for $C_3/C_4$ plant* |
| $F_{ca}$ | $\mu mol\, m^{-2}\, s^{-1}$ | $CO_2$ flux above land surface |
| $F_{cs}$ | $\mu mol\, m^{-2}\, s^{-1}$ | $CO_2$ flux from the soil surface |
| $F$ | $m^2\, m^{-2}$ | Canopy leaf area index |
| $F_{shd}$ | $m^2\, m^{-2}$ | Shaded leaf area index |
| $F_{slt}$ | $m^2\, m^{-2}$ | Sunlit leaf area index |
| $f_d$ | | Fraction of diffusive radiation in total radiation |
| $f(\psi)$ | | Adjustment factor to count for soil moisture effect |

**Appendix A.** (*Continued*)

| Symbol | Units | Definition |
|---|---|---|
| $G(\mu)$ | | Projection of leaves in direction of incoming radiation flux* |
| $g_b$ | $\mu mol\, m^{-2}\, s^{-1}$ | Leaf boundary layer aerodynamic conductance |
| $g_s$ | $\mu mol\, m^{-2}\, s^{-1}$ | Stomatal conductance to latent and sensible heat transfer |
| $\Gamma_*$ | $\mu mol\, mol^{-1}$ | The $CO_2$ compensation point of the leaves* |
| $\gamma$ | $Pa\, K^{-1}$ | Psychometric constant |
| $h_s$ | | Relative humidity within the leaf surface boundary layer |
| $K_c$ | $\mu mol\, mol^{-1}$ | Michaelis-Menten competitive inhibition constant for $CO_2$* |
| $K_o$ | $\mu mol\, mol^{-1}$ | Michaelis–Menten competitive inhibition constant for $O_2$* |
| $\bar{k}$ | | Time-mean value of radiation extinction coefficient* |
| $m$ | | Coefficient in Eq. (3) (9 for $C_3$, 4 for $C_4$ vegetation) |
| $N$ | | Canopy green leaf fraction |
| $O_i$ | $\mu mol\, mol^{-1}$ | Internal $O_2$ concentration of the leaves |
| $P$ | | Interim variables for the analytic solutions |
| PAR, $PAR_0$ | $\mu mol\, m^{-2}\, s^{-1}$ | Photosynthetically active radiation above the canopy |
| $PAR_{dr}$ | $\mu mol\, m^{-2}\, s^{-1}$ | Direct photosynthetically active radiation above the canopy |
| $PAR_{df}$ | $\mu mol\, m^{-2}\, s^{-1}$ | Diffusive photosynthetically active radiation above the canopy |
| $PAR_{slt}$ | $\mu mol\, m^{-2}\, s^{-1}$ | PAR received by sunlit leaves |
| $PAR_{shd}$ | $\mu mol\, m^{-2}\, s^{-1}$ | PAR received by shaded leaves |
| $p$ | Pa | Air pressure |
| $\psi$ | Pa | Soil water potential |
| $\Pi$ | | Leaf to canopy scaling factor (see Eq. (12)) |
| $Q$ | | Interim variables for the analytic solutions |
| $R_d$ | $\mu mol\, m^{-2}\, s^{-1}$ | The dark respiration rate of the canopy |
| $r_a$ | | Aerodynamic resistance of the air above the canopy to the measurement height |
| $\rho c_p$ | $J\, m^{-3}\, K^{-1}$ | Volumetric heat capacity of air |
| $T_a$ | °C | Air temperature at the reference height |
| $T_c$ | °C | Integrated leaf temperature of the canopy |
| $\theta_s$ | ° | Sun elevation angle |
| $\theta_{ls}$ | ° | Mean angle between leaf normal and sunlight |
| $\mu$ | | Direction of incoming radiation flux |
| $V_{max}$ | $\mu mol\, m^{-2}\, s^{-1}$ | Maximum RuBP carboxylation rate |
| $V$ | | Canopy cover fraction |
| $W_c$ | $\mu mol\, m^{-2}\, s^{-1}$ | Rubisco-limited rate of $CO_2$ assimilation |
| $W_e$ | $\mu mol\, m^{-2}\, s^{-1}$ | Electron transportation limited $CO_2$ assimilation rate |
| $W_s$ | $\mu mol\, m^{-2}\, s^{-1}$ | Product sink limited rate of $CO_2$ assimilation |
| $\omega_\Pi$ | | Leaf-scattering coefficient for PAR (Sellers et al., 1996a) |

## Appendix B. Analytical solutions of Eq. (14)

In Eq. (14)

$$A = A_3A_6mh_sg_b^2p + A_3B_1bg_bF \quad (A.1)$$

$$B = g_bp(A_6((1.6 - mh_s)B_1 + A_4mh_sg_b) + A_3A_7mh_sg_b) + bF(A_4B_1g_b + A_3B_2g_b - B_1^2) \quad (A.2)$$

$$C = g_bp(A_6(1.6 - mh_s)B_2 + A_7(1.6 - mh_s)B_1 + A_4mh_sg_b) + bF(A_4B_2g_b - 2B_1B_2) \quad (A.3)$$

$$D = A_7B_2(1.6 - mh_s)g_bp - B_2^2bF \quad (A.4)$$

and

$$A_6 = A_1 + A_3A_5 \quad (A.5)$$

$$A_7 = A_4A_5 - A_1A_2 \quad (A.6)$$

$$B_1 = C_ag_bA_3 - 1.4pA_6 \quad (A.7)$$

$$B_2 = C_ag_bA_4 - 1.4pA_7 \quad (A.8)$$

$$h_s = e_s/e_s^*(T_c) \quad (A.9)$$

If we define $P = (C/A) - (B^2/3A^2)$ and $Q = (D/A) + (2B^3/27A^3) - (BC/3A^2)$, then the discriminator of Eq. (14) is

$$\Delta = \left(\frac{Q}{2}\right)^2 + \left(\frac{P}{3}\right)^3 \quad (A.10)$$

If ($\Delta \geq 0$), the cubic Eq. (14) has only one valid solution. If ($\Delta < 0$), Eq. (14) yields three roots. These roots can be computed with equations listed in most mathematical handbooks. The valid solution is the positive minimum of the three, that is

$$C_i = \min(x_1, x_2, x_3) \quad (A.11)$$

If $A_1 \neq 0$ and $A_3 = 0$ in Eq. (13), Eq. (14) becomes the following quadratic equation:

$$a_cC_i^2 + b_cC_i + c_c = 0 \quad (A.12)$$

where

$$a_c = g_bpA_1(1.4pA_1(1.6 - mh_s) - mh_sg_b) + bF(1.4pA_1(1.4pA_1 + g_b)) \quad (A.13)$$

$$b_c = -g_bpA_1 1.4pA_1(C_ag_b - 1.4pA_5) + A_5g_bp(1.4pA_1(1.6 - mh_s) - mh_sg_b) + bF(2.8pA_1 + g_b)(C_ag_b - 1.4pA_5) \quad (A.14)$$

$$c_c = -g_bpA_5(1.6 - mh_s)(C_ag_b - 1.4pA_5) + bF(C_ag_b - 1.4pA_5)^2 \quad (A.15)$$

The discriminator of Eq. (A.12) is

$$\Delta_2 = b_c^2 - 4a_cc_c \quad (A.16)$$

When ($\Delta_2 \geq 0$), the quadratic equation has two roots. These two roots can be computed with equations listed in most mathematical handbooks. The minimum of them is the valid value for $C_i$ if it is greater than zero, that is

$$C_i = \min(x_1, x_2) \quad (A.17)$$

If $\Delta_2 < 0$, then the equation has no valid solutions.

## References


Baldocchi, D., 1994. An analytical solution for coupled leaf photosynthesis and stomatal conductance models. Tree Physiol. 14, 1069–1079.

Ball, J.T., 1988. An Analysis of Stomatal Conductance. Ph.D. Dissertation, Stanford University, Stanford, CA, 89 p.

Bastable, H.G., Shuttleworth, W.J., Dallarosa, R.L.G., Fisch, G., Nobre, C.A., 1993. Observations of climate, albedo, and surface radiation over cleared and undisturbed Amazonian forest. Int. J. Climatol. 13, 783–798.

Bonan, G.B., 1995. Land-atmosphere $CO_2$ exchange simulated by a land surface process model coupled to an atmospheric general circulation model. J. Geophys. Res. 100, 2817–2831.

Boonen, C., Samson, R., Janssens, K., Pien, H., Lemeur, R., Berckmans, D., 2002. Scaling the spatial distribution of photosynthesis from leaf to canopy in a plant growth chamber. Ecol. Model. 156 (2/3), 201–212.

Chen, J.M., Liu, J., Cihlar, J., Goulden, M.L., 1999. Daily canopy photosynthesis model through temporal and spatial scaling for remote sensing applications. Ecol. Model. 124, 99–119.

Chou, S.C., Tanajura, C.A.S., Xue, Y., Nobre, C.A., 2002. Simulations with the coupled Eta/SSiB model over South America. J. Geophys. Res., submitted for publication.

Collatz, G.J., Grivet, C., Ball, J.T., Berry, J.A., 1991. Physiological and environmental regulation of stomatal conductance, photosynthesis and transpiration: a model that includes a laminar boundary layer. Agric. For. Meteor. 54, 107–136.

Collatz, G.J., Ribas-Carbo, M., Berry, J.A., 1992. Coupled photosynthesis-stomatal conductance model for leaves of $C_4$ plants. Aust. J. Plant Physiol. 19, 519–538.

Cox, P.M., Betts, R.A., Jones, C.D., Spall, S.A., Totterdell, I.J., 2000. Acceleration of global warming due to carbon cycle feedbacks in a coupled climate model. Nature 408, 184–187.

Denning, A.S., Collatz, G.J., Zhang, C., Randall, D.A., Berry, J.A., Sellers, P.J., Colello, G.D., Dazlich, D.A., 1996a. Simulations of terrestrial carbon metabolism and atmospheric $CO_2$ in a general circulation model. Part I. Surface carbon fluxes. Tellus 48B, 521–542.

Denning, A.S., Randall, D.A., Collatz, G.J., Sellers, P.J., 1996b. Simulations of terrestrial carbon metabolism and atmospheric $CO_2$ in a general circulation model. Part 2. Simulated $CO_2$ concentration. Tellus 48(B), 543–567.

Fan, S.-M., Wofsy, S., Bakwin, P., Jacob, D., 1995. Atmospheric-biosphere exchange of $CO_2$ and $O_3$ in the central Amazon forest. J. Geophys. Res. 95, 16851–16864.

Farquhar, G.D., von Caemmerer, S., Berry, J.A., 1980. A biochemical model of photosynthetic $CO_2$ assimilation in leaves of $C_3$ species. Planta 149, 78–90.

Gash, J.H.C., Nobre, C.A., Roberts, J.M., Victoria, R.L., 1996. Amazonian Deforestation and Climate. Wiley, Chichester, 611 p.

Henderson-Seller, A., Yang, Z.-L., Dickinson, R.E., 1993. The project for intercomparison of land-surface parameterization schemes. Bull. Am. Meteor. Soc. 74, 1335–1349.

Henderson-Seller, A., Pitman, A.J., Love, P.K., Irannejad, P., Chen, T.H., 1995. The project for intercomparison of land-surface parameterization schemes (PILPS): phases 2 and 3. Bull. Am. Meteor. Soc. 76, 489–503.

Houghton, R.A., Skole, D.L., Nobre, C.A., 2000. Annual fluxes or carbon from deforestation and regrowth in the Brazilian Amazon. Nature 403 (6767), 301–304.

Jarvis, P.G., 1976. The interpretation of the variations in leaf water potential and stomatal conductance found in canopies in the field. Phil. Trans. R. Soc. Lond. Ser. B Biol. Sci. 273, 593–610.

Jorgensen, S.E., 1997. Ecological modelling by "Ecological Modelling". Ecol. Model. 100 (1/3), 5–10.

Keller, M., Melillo, J., Zamboni de Mello, W., 1997. Trace gas emissions from ecosystems of the Amazon basin. Ciência e Cultura J. Brazilian Assoc. Adv. Sci. 49, 87–97.

Keller, M., Palace, M., Hurtt, G., 2001. Biomass estimation in the tapajos National forest, Brazil: examination of sampling and allometric uncertainties. For. Ecol. Manage. 154 (3), 371–382.

Malhi, Y., Nobre, A.D., Grace, J., Kruijt, B., Pereira, M.G.P., Culf, A., Scott, S., 1998. Carbon dioxide transfer over a central Amazonian rain forest. J. Geophy. Res. 103 (D24), 31593–31612.

McWilliams, A.L.C., Roberts, J.M., Cabral, O.M.R., Leitao, M.V.B.R., de Costa, A.C.L., Maitelli, G.T., Zamporoni, C.A.G.P., 1993. Leaf area index and above ground biomass of terra firm rain forest and adjacent clearings in Amazonia. Funct. Ecol. 7 (3), 310–317.

Moncrieff, J.B., Massheder, J.M., de Bruin, H., Elbers, J., Friborg, T., Huesunkveld, B., Kabat, P., Scott, S., Soegaard, H., Verhoef, A., 1997. A system to measure surface fluxes of momentum, sensible heat, water vapor and carbon dioxide. J. Hydrol. 188/189, 589–611.

Moore, C.J., 1986. Frequency response corrections for Eddy correlation systems. Boundary Layer Meteor. 37, 17–35.

Norman, J.M., 1982. Simulation of Microclimates. Biometeorology in Integrated Pest Management. Academic Press, New York, pp. 65–69.

Phillips, O.L., Malhi, Y., Higuchi, N., Laurance, W.F., Nunez, P.V., Vasquez, R.M., Laurance, S.G., Ferreira, L.V., Stern, M., Brown, S., Grace, J., 1998. Changes in the carbon balance of tropical forests: evidence from long-term plots. Science 282 (5388), 439–442.

Schimel, D.S., House, J.I., Hibbard, K.A., Bousquet, P., Ciais, P., Peylin, P., Braswell, B.H., Apps, M.J., Baker, D., Bondeau, A., Canadell, J., Churkina, G., Cramer, W., Denning, A.S., Field, C.B., Friedlingstein, P., Goodale, C., Heimann, M., Houghton, R.A., Melillo, J.M., Moore, B., Murdiyarso, D., Noble, I., Pacala, S.W., Prentice, I.C., Raupach, M.R., Rayner, P.J., Scholes, R.J., Steffen, W.L., Wirth, C., 2001. Recent patterns and mechanisms of carbon exchange by terrestrial ecosystems. Nature 414, 169–172.

Sellers, P.J., Berry, J.A., Collatz, G.J., Field, C.B., Hall, F.G., 1992. Canopy reflectance, photosynthesis and transpiration. Part III. A reanalysis using enzyme kinetics-electron transport models of leaf physiology. Remote Sens. Environ. 42, 187–216.

Sellers, P.J., Randall, D.A., Collatz, G.J., Berry, J.A., Field, C.B., Dazlich, D.A., Zhang, C., Collelo, G.D., Bounoua, L., 1996a. A revised land surface parameterization (SSiB_2) for atmospheric GCMs. Part I. Model formulation. J. Climate 9, 676–705.

Sellers, P.J., Bounoua, L., Collatz, G.J., Randal, D.A., Dazlich, D.A., Los, S.O., Berry, J.A., Fung, I., Tucker, C.J., Field, C.B., Jensen, T.G., 1996b. Comparison of radiative and physiological effects of doubled atmospheric $CO_2$ on climate. Science 271, 1402–1406.

Sellers, P.J., Dickinson, R.E., Randall, D.A., Betts, A.K., Hall, F.G., Berry, J.A., Collatz, G.J., Denning, A.S., Mooney, H.A., Nobre, C.A., Sato, N., Field, C.B., Henderson-Sellers, A., 1997. Modeling the exchanges of energy, water, and carbon between continents and the atmosphere. Science 275 (5299), 502–509.

Shuttleworth, W.J., Gash, J.H.C., Roberts, J.M., Nobre, C.A., Molion, L.C.B., Ribeiro, M.N.G., 1991. Post-deforestation Amazonian climate: Anglo-Brazilian research to improve prediction. J. Hydrol. 129, 71–86.

Thornley, J.H.M., Johnson, I.R., 1990. Plant and Crop Modelling. Oxford University Press, Oxford, 669 p.

Tian, H., Melillo, J.M., Kicklighter, D.W., McGuire, A.D., Helfrich, J., Moore, B., Vorosmarty, C.J., 2000. Climatic and biotic controls on annual carbon storage in Amazonian ecosystems. Global Ecol. Biogeography 9, 315–335.

Williams, M., Malhi, Y., Nobre, A.D., Rastetter, E.B., Grace, J., Pereira, M.G.P., 1998. Seasonal variation in net carbon exchange and evapotranspiration in a Brazilian rain forest: a modelling analysis. Plant, Cell Environ. 21, 953–968.

Wright, I.R., Gash, J.H.C., Rocha, H.R., Shuttleworth, W.J., Nobre, C.A., Carvalho, P.R.A., Leitao, M.V.B.R., Maitelli, G.T., Zamparoni, C.A.G.P., 1992. Dry season micrometeorology of Amazonian ranchland. Quart. J. Roy. Meteor. Soc. 118, 1083–1099.

Xue, Y., Sellers, P.J., Kinter III, J.L., Shukla, J., 1991. A simplified biosphere model for global climate studies. J. Climate 4, 345–364.

Xue, Y., Bastable, H.G., Dirmeyer, P.A., Sellers, P.J., 1996a. Sensitivity of simulated surface fluxes to changes in land surface parameterization—a study using ABRACOS data. J. Appl. Meteor. 35, 386–400.

Xue, Y., Zeng, F.J., Schlosser, C.A., 1996b. SSiB and its sensitivity to soil properties—a case study using HAPEX-Mobilhy data. Global Planetary Change 13, 183–194.

Xue, Y., Sellers, P.J., Zeng, F.J., Schlosser, C.A., 1997. Comments on "Use of midlatitude soil moisture and meteorological observations to validate soil moisture simulations with biosphere and bucket models". J. Climate 10, 374–376.

Xue, Y., Zeng, F.J., Mitchell, K., Janjic, Z., Rogers, E., 2001. The impact of land surface processes on the simulation of the US hydrological cycle: a case study of US 1993 flood using the Eta/SSiB regional model. Mon. Wea. Rev. 129, 2833–2860.